

**ONLINE SUPPLEMENT:**

**ADENOSINE ACTIVATES A<sub>2b</sub> RECEPTORS AND ENHANCES CHLORIDE  
SECRETION IN KIDNEY INNER MEDULLARY COLLECTING DUCT CELLS**

Madhumitha Rajagopal and Alan C. Pao

Division of Nephrology, Department of Medicine, Stanford University, Stanford,  
California 94305

Short Title: Adenosine Induces Chloride Secretion in IMCD Cells

Corresponding Author:

Alan C. Pao, M.D.

Division of Nephrology, Department of Medicine, Stanford University

780 Welch Road, Suite 106

Palo Alto, CA 94304

Tel: (650) 721-2245; Fax: (650) 721-3161

Email: paoman@stanford.edu

## EXPANDED METHODS

### *Ussing Chamber Measurements*

Cell sheets were mounted between the Lucite half chambers of the Ussing chamber apparatus and bathed in Krebs-Henseleit solution (in mmol/L: 140 NaCl, 25 NaHCO<sub>3</sub>, 5 KCl, 5 glucose, 2 CaCl<sub>2</sub>, and 1 MgCl<sub>2</sub>) and gassed with a mixture of 95% O<sub>2</sub> and 5% CO<sub>2</sub>. Transepithelial voltage ( $V_{te}$ ) across cell sheets was clamped to 0 mV, and a set voltage pulse of 1 mV was applied across cell sheets for 200 ms every 20 s. The short-circuit current ( $I_{sc}$ ) and transepithelial resistance ( $R_{te}$ ) across cell sheets were continuously recorded using Acquire and Analyze Software (Physiological Instruments, San Diego, CA).

### *Western Blot Analysis*

Seventy micrograms of protein from mIMCD-K2 lysates were resolved by 12% SDS-PAGE and transferred to PVDF membranes (BioRad, Hercules, CA). The membranes were immunostained with 1 µg/ml of anti-A2b receptor antibody (Alpha Diagnostics International, San Antonio, TX) for detection of A2b receptor immunoreactive protein. Membranes were incubated with horseradish peroxidase conjugated-secondary antibody (Amersham Biosciences, Piscataway, NH) and processed, as described previously<sup>1</sup>.

### *cAMP Assay*

Intracellular cAMP levels were measured using the Parameter cAMP ELISA assay kit (R & D Systems, Minneapolis, MN) after the apical side of cell sheets were treated with 10<sup>-5</sup> mol/L adenosine or vehicle control. Cell sheets containing ~ 10<sup>6</sup> cells were lysed, and cAMP concentrations were determined per manufacturer instructions.

## REFERENCES

1. Pao AC, McCormick JA, Li H, Siu J, Govaerts C, Bhalla V, Soundararajan R, Pearce D. NH<sub>2</sub> terminus of serum and glucocorticoid-regulated kinase 1 binds to phosphoinositides and is essential for isoform-specific physiological functions. *Am J Physiol Renal Physiol.* 2007;292:F1741-1750.
2. Hall DA, Varney DM. Effect of vasopressin on electrical potential difference and chloride transport in mouse medullary thick ascending limb of Henle's loop. *J Clin Invest.* 1980;66:792-802.
3. Kriz W, Koepsell H. The structural organization of the mouse kidney. *Z Anat Entwicklungsgesch.* 1974;144:137-163.
4. Mejia R, Sands JM, Stephenson JL, Knepper MA. Renal actions of atrial natriuretic factor: a mathematical modeling study. *Am J Physiol.* 1989;257:F1146-1157.
5. Dickinson H, Moritz K, Wintour EM, Walker DW, Kett MM. A comparative study of renal function in the desert-adapted spiny mouse and the laboratory-adapted C57BL/6 mouse: response to dietary salt load. *Am J Physiol Renal Physiol.* 2007;293:F1093-1098.
6. Daly JW, Padgett WL. Agonist activity of 2- and 5'-substituted adenosine analogs and their N6-cycloalkyl derivatives at A1- and A2-adenosine receptors coupled to adenylate cyclase. *Biochem Pharmacol.* 1992;43:1089-1093.
7. Peakman MC, Hill SJ. Adenosine A2B-receptor-mediated cyclic AMP accumulation in primary rat astrocytes. *Br J Pharmacol.* 1994;111:191-198.
8. Yaar R, Jones MR, Chen JF, Ravid K. Animal models for the study of adenosine receptor function. *J Cell Physiol.* 2005;202:9-20.
9. Zhou QY, Li C, Olah ME, Johnson RA, Stiles GL, Civelli O. Molecular cloning and characterization of an adenosine receptor: the A<sub>3</sub> adenosine receptor. *Proc Natl Acad Sci U S A.* 1992;89:7432-7436.
10. Klotz KN. Adenosine receptors and their ligands. *Naunyn Schmiedebergs Arch Pharmacol.* 2000;362:382-391.
11. Ongini E, Dionisotti S, Gessi S, Irenius E, Fredholm BB. Comparison of CGS 15943, ZM 241385 and SCH 58261 as antagonists at human adenosine receptors. *Naunyn Schmiedebergs Arch Pharmacol.* 1999;359:7-10.
12. Moresco RM, Todde S, Belloli S, Simonelli P, Panzacchi A, Rigamonti M, Galli-Kienle M, Fazio F. In vivo imaging of adenosine A<sub>2A</sub> receptors in rat and primate brain using [<sup>11</sup>C]SCH442416. *Eur J Nucl Med Mol Imaging.* 2005;32:405-413.
13. Borrmann T, Hinz S, Bertarelli DC, Li W, Florin NC, Scheiff AB, Muller CE. 1-alkyl-8-(piperazine-1-sulfonyl)phenylxanthines: development and characterization of adenosine A<sub>2B</sub> receptor antagonists and a new radioligand with subnanomolar affinity and subtype specificity. *J Med Chem.* 2009;52:3994-4006.

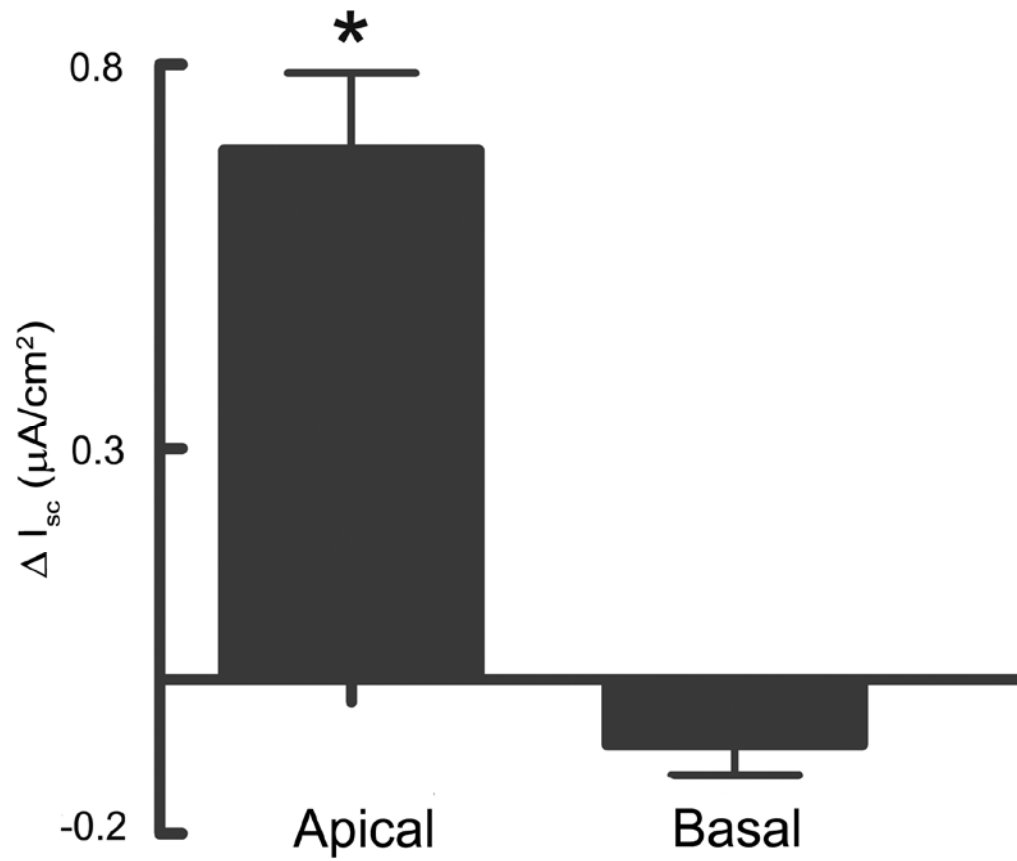
**Table S1.** Affinity of adenosine receptor agonists and antagonists for the four classes of adenosine receptors.

---

Agonist/Antagonist	K <sub>i</sub> values (nmol/L)				References
	A1	A2a	A2b	A3	
Adenosine	73	150	5100	6500	6-9
CPA	2.3	790	18,600	43	10
CGS21680	290	27	89,000	67	10
NECA	14	20	2400	6.2	10
DPCPX	3.9	130	1000	4000	10
ZM241385	255	0.8	50	>10,000	11
SCH442416	1111	0.048	>10,000	>10,000	12
PSB 603	>10,000	>10,000	0.568	>10,000	13

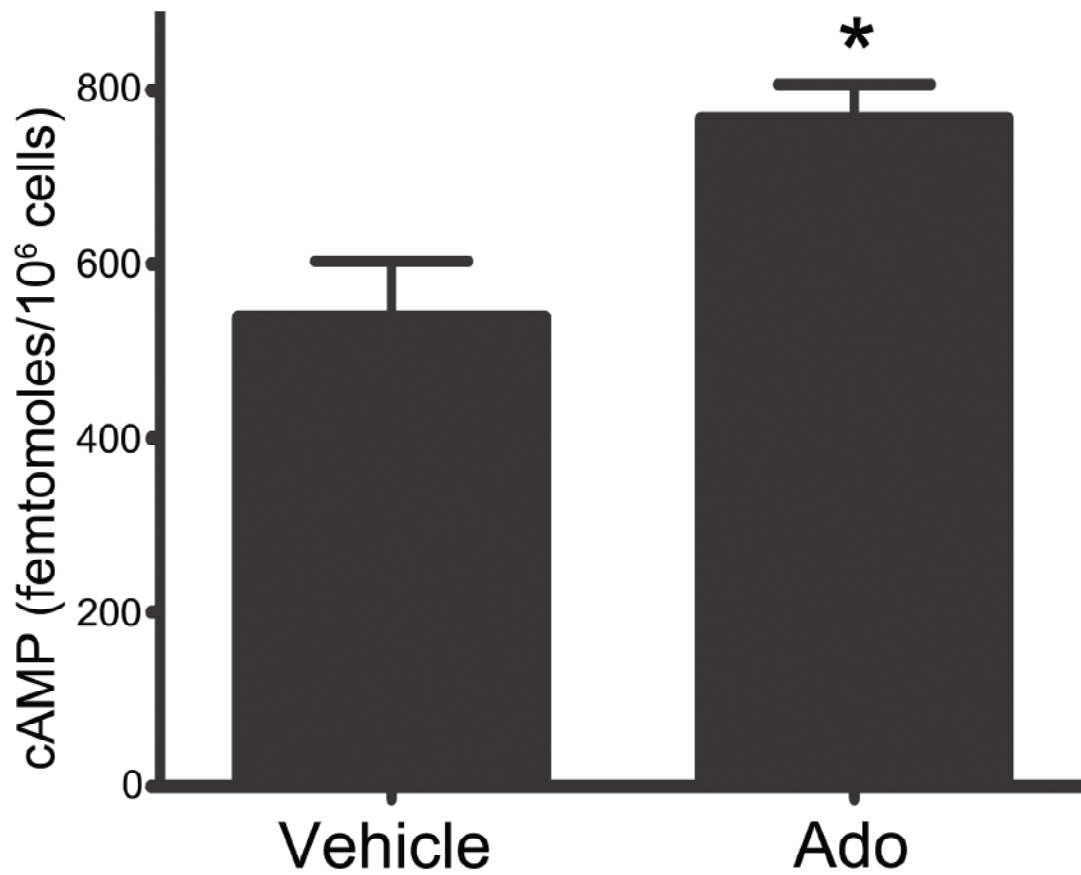
---

Figure S1



**Figure S1.** Sidedness of adenosine-induced  $I_{sc}$  across mIMCD-K2 cell sheets. Adenosine was added to either the apical or the basal side of paired cell sheets mounted in an Ussing chamber.  $\Delta I_{sc}$ , change in  $I_{sc}$ . Values are mean  $\pm$  SE (n = 13 filters). \*P < 0.05.

Figure S2



**Figure S2.** Effect of apical adenosine treatment on intracellular cAMP levels in mIMCD-K2 cells. Cell sheets treated with apical adenosine  $10^{-5}$  mol/L (Ado) had significantly higher intracellular cAMP levels than cells treated with vehicle control. Values are mean  $\pm$  SE (n = 6 cell sheets). \*P < 0.05.

## Figure S3

### Estimated surface area of mouse IMCD

Single collecting duct:

Internal diameter = 20  $\mu\text{m}$  [2]

Length = 5.3 mm = 5300  $\mu\text{m}$  [3]

$$2\pi rh = 2 \times \pi \times 10 \mu\text{m} \times 5300 \mu\text{m} = 333,142.8 \mu\text{m}^2 = 0.3331428 \text{ mm}^2$$

The number of collecting ducts per kidney in a rodent model = 10,000 [4]

Surface area of mouse IMCD:

$$0.3331428 \text{ mm}^2 \times 10,000 \text{ collecting ducts} \times 2 \text{ kidneys} = 6662.856 \text{ mm}^2 \\ = 66.63 \text{ cm}^2$$

### Estimated $\text{Cl}^-$ flux across mouse IMCD epithelium per day

Typical  $I_{\text{sc}}$  increase with  $10^{-5}$  mol/L adenosine = 1.2  $\mu\text{A}/\text{cm}^2$

$I_{\text{sc}}$  increase across mouse IMCD epithelium = 1.2  $\mu\text{A}/\text{cm}^2 \times 66.63 \text{ cm}^2 = 80 \mu\text{A}$

Using Faraday's constant, 26  $\mu\text{A} = 1 \mu\text{Eq}/\text{hr}$ , 80  $\mu\text{A} = 3.07 \mu\text{Eq}/\text{hr}$

3.07  $\mu\text{Eq}/\text{hr} \times 24 \text{ hrs} = 74 \mu\text{Eq}$  of  $\text{Cl}^-$  secreted across mouse IMCD epithelium

### Estimated Effect on Daily Fractional Excretion of Chloride ( $\text{FE}_{\text{Cl}}$ )

Filtered  $\text{Cl}^-$  load in one day:

Serum  $[\text{Cl}^-] = 110 \text{ mEq}/\text{L} = 110 \mu\text{Eq}/\text{mL}$

Creatinine clearance in a C57BL/6 mouse under high salt diet = 179  $\mu\text{L}/\text{min}$  [5]

$110 \mu\text{Eq}/\text{mL} \times 1 \text{ mL}/1000 \mu\text{L} \times 179 \mu\text{L}/\text{min} \times 1440 \text{ min} = 28,354 \mu\text{Eq}$   $\text{Cl}^-$  filtered

$$\text{FE}_{\text{Cl}} = 74 \mu\text{Eq} \text{ of } \text{Cl}^- \text{ secreted} / 28,354 \mu\text{Eq} \text{ } \text{Cl}^- \text{ filtered} = 0.261\%$$

**Figure S3.** Mathematical modeling of the magnitude of adenosine-stimulated chloride flux extrapolated to the *in vivo* setting. Calculations listed are for the estimated adenosine-stimulated chloride flux across mouse IMCD epithelium and the estimated effect of adenosine-stimulated chloride secretion in the IMCD on daily fractional excretion of chloride ( $\text{FE}_{\text{Cl}}$ ).